Opinion Vol. 13, No. 11 / 1 Nov 2023 / Optical Materials Express 3045
Optical Materials EXPRESS

Near-field quantum nanoscopy in the far-infrared enabled by quantum cascade lasers: opinion

MIRIAM SERENA VITIELLO

NEST, CNR - Istituto Nanoscienze and Scuola Normale Superiore, Piazza San Silvestro 12, 56127, Pisa, Italy

Abstract: In this opinion article, I summarize some of the recent developments in the field of near-field nanoscopy of quantum materials in the far-infrared, highlighting the key role of the quantum cascade laser as a tool for building up unique near-field microscopes for mapping material and devices at the nanoscale, in a phase-sensitive, detectorless configuration, and I provide opinion on some of potential challenges and opportunities in the field.

1. Introduction

Near-field nanoscopy at terahertz (THz) frequencies (0.1-10 THz, 3mm-3μm wavelength) has been growing intensely in the past 20 years, making the field incredibly broad [1]. It enables studies of object within a very large span of scales, from the wavelength scale (300 μm) to the nanometer scale; it had to be adapted to a broad range of instrumentations, promoting the development of a broad range of near-field probes (aperture-limited probes as fiber or hollow tips, or metal or silicon tips for which the resolution is wavelength independent) that can be used for imaging [1]. These developments offered unexpected opportunities. While it may be logical to have one instrument that fits all purposes, there is no universal THz near-field solution that is capable to address all the applications. The diversity of the field has been beneficial so far to the development and the understanding of the capabilities and limitation of the different near-field approaches. Presently, there is indeed choice which method to use for a given application, hence endorsing near-field THz nanoscopy as an universal tool for mapping waveguide and resonators-modes [2], metasurfaces [3] and bio-tissues [4] (over mm^2 areas) or nanowires [5], quantum dots [6], and photoexcited electromagnetic modes as plamons [7,8], plasmon-polaritons [9], excitons [10], or phonon polaritons [11,12] (over nanometer scales).

So far, THz scattering scanning near-field optical microscopy (s-SNOM) has been performed using broadband sources, such as those used in time domain TDS systems, that show a performance drop at frequencies > 1.8 THz [13], and only allow slow data acquisition rates (14 sec/pixel) [13], gas lasers [14], or bulky (not table-top) and high-cost free electron lasers [15], or, alternatively, sub-THz electronic sources, [16] or THz quantum cascade lasers (QCLs) emitting only one discrete frequency in a phase-sensitive detectorless configuration [17–19]. The main disadvantages of broadband THz sources are their cumbersome setups, which require an external laser to generate ultrashort pump pulses, their limited (μW) output-powers and the need of sensitive THz detectors, whilst electronic sources and gas lasers only operate on specific modes, and are usually neither compact nor high power. In contrast, when THz QCLs are used for THz nanoscopy, they are powerful, do not require a separate detector, and can be eventually operated in a multi-frequency configuration, either with a few random emitted modes [19], or in a frequency comb configuration, with a sequence of multiple phase locked modes [20]. The right choice of an appropriate method in THz microscopy is critical.

Here, I discuss the potential of a series of near-field nanoimaging approaches that, while exploiting the same core building block (a detectorless QCL-based nanoscope) [17], rely on

#504097 https://doi.org/10.1364/OME.504097
Journal © 2023 Received 23 Aug 2023; revised 30 Aug 2023; accepted 30 Aug 2023; published 2 Oct 2023

Optical Materials EXPRESS

different physical mechanism for imaging reconstruction and I highlight their potential for mapping bi-dimensional (2D) and one-dimensional nanomaterials and devices.

2. Detectorless near-field nanoscopy

The core operational mechanism of QCL-based THz s-SNOM is self-mixing interferometry (SMI) [21,22]. The basic concept of self-mixing was discovered soon after laser invention. The reinjection of a small part (10^{-4}-10^{-2}) of the emitted field produces coherent nonlinear interference in the laser cavity and is enough to significantly perturb the laser. This is typically annoying, so the benefits are counterintuitive: all laser parameters (voltage, threshold current, emitted power, laser linewidth) are perturbed. However, this also makes a laser source capable of sensing its external environment. The process is also inherently fast (>GHz acquisition rates) since the maximum response speed to optical feedback is determined by the frequency of the relaxation oscillations in the laser, and sensitive (noise-equivalent-powers < 10 pW/Hz$^{1/2}$). In THz-QCLs, indeed, the lifetime of the upper laser state is limited by elastic and inelastic scattering mechanisms to 5–10 ps [23], enabling, in principle, response frequencies of the order of 100 GHz. Coherent superposition of re-injected THz field with the QCL intracavity field produces a perturbation of the laser voltage ΔV that depends on both the amplitude and the phase of the THz field scattered by the tip, hence allowing to reconstruct the near field maps [17–19].

The simple architecture of SMI can be described in a three-cavity model employing the Lang-Kobayashi (LK) theory [24,25], in which two coupled differential equations describe the evolution of the excited state population $N(t)$ and the optical field $E(t)$. SMI arises from this term which changes the field amplitude and phase and contains the target reflectivity R and the external cavity length. The LK equations read [24]:

$$\frac{dE(t)}{dt} = \frac{1}{2}(1 + i\alpha_H)\left[G_n(N(t) - N_0) - \frac{1}{\tau_p}\right]E(t) + \frac{\gamma}{\tau_c}E(t - \tau)e^{-i\omega_0\tau} \quad (1)$$

$$\frac{dN(t)}{dt} = \frac{J\eta}{qd} - \frac{N(t)}{\tau_e} - G_n(N(t) - N_0)|E(t)|^2 \quad (2)$$

where N_0 is the carrier density at transparency, G_n is the gain coefficient, $\tau = 2\,L/c$, τ_p and τ_c are the photon life time and the cavity round trip time inside the QCL cavity, respectively, and τ_e is the carriers decay time ($1 - 10\ ps$), J is the current density, η is the internal quantum efficiency, d is the active layer thickness and q is the electron charge, γ is the feedback strength parameter which depends on R, i.e. the fraction of the back-scattered field that efficiently couples with the lasing mode which depends of the target reflectivity and, α_H is the linewidth enhancement factor. The analysis of the near-field signals can be performed through the Lang–Kobayashi formalism under very different operational conditions, ranging from the very weak (C < 0.1) to the weak (0.1 < C < 1) feedback regimes [19]. Very interesting, the more-complex non-sinusoidal line shape of the self-mixing fringes, the best imaging conditions in terms of the signal to noise ratio (SNR), are obtained in the high feedback regime. A first-order approximated method is used to evaluate the self-mixing signal phase and amplitude even for non-sinusoidal fringes, allowing for an efficient, in terms of scan speed, and reliable image reconstruction [19].

2.1. Mapping 2D nanomaterials

Nanoscopy in the SMI configuration can allow to probe modal characteristics and photoexcited modes, at multiple wavelengths, with a resolution set by the tip radius (30-250 μm). This can be done by mounting on the same chip a set of single-mode THz QCLs operating at different wavelengths (λ)/frequencies in the 1.5-5.0 THz range, with a polarization parallel to the tip. In order to sample the SM fringes and retrieve the phase shift experienced by the field in the scattering process, the length L of the external cavity, formed by the tip and output laser facet, can

Optical Materials EXPRESS

be varied up to distances $>2\lambda = 4\pi c/\omega_0$ with a delay line built on a linear translation stage with a sub-μm spatial resolution (Fig. 1(a)). 2D materials can be scanned along a line orthogonal to the substrate-material edge. The amplitude of the self-mixing signal at high demodulation orders $n \geq 3$, as a function of the distance between the tip and the output laser facet L, and of the position on the sample, labeled as x, can be extrapolated by analyzing the self-mixing fringes at each x with sinusoidal fit functions, together with the phase ϕ_n along the scan trajectory. With this approach it is also possible to image signal intensity modulations in regions on flat topography, which can provide signature of interference of propagating modes launched by the tip and reflected at the flake edges [26]. This approach has been recently applied to map topological insulators as $Bi_2Se_{2.2}Te_{0.8}$ and Bi_2Se_3 of different thicknesses (20-120 nm) allowing to identify hyperbolic plasmon–phonon-polaritons modes at THz frequencies, and massive bulk plasmons associated to band bending induced 2D electron gas, respectively [26].

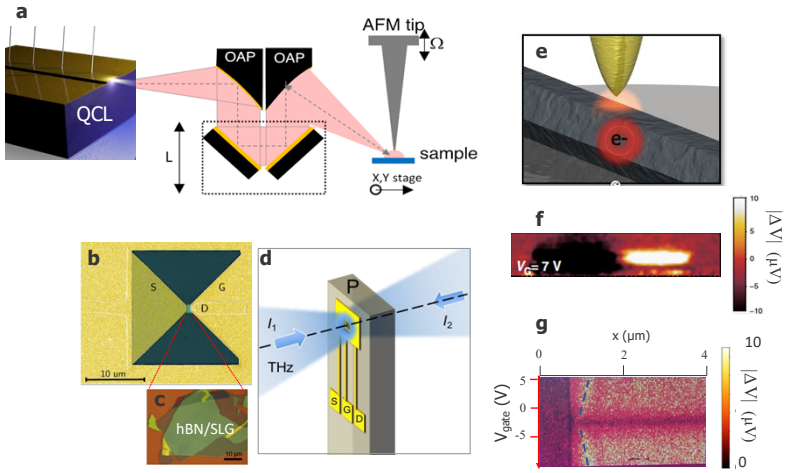

Fig. 1. **a.** Schematic of a QCL based detectorless near field optical microscope; **b-c**. Scanning electron microscope image of a near-field probe with a 20 μm aperture and an embedded heterostructure of hBN/single layer graphene (SLG). **d.** Schematics of a THz near-field probe with an embedded 2D material transistor, front- and back- illuminated in an interferometric near field set-up. **e.** Schematics of photocurrent THz nanoscopy on a semiconductor nanowire. **f-g**. Near-field photovoltage map in a nanowire (f) [5] and graphene (g) field effect transistor (FET) collected at zero source-drain bias and at gate voltage $V_G = 7$ V(f) or at different V_G (g). The V_G-dependent acoustic plasmon propagating in the graphene FET is marked by dashed blue lines.

3. Hyperspectral nanoscopy based on QCL frequency combs

A hyperspectral, detectorless, s-SNOM imaging system at frequencies in the 2-5 THz range, can be built by employing a high power (~10 mW) excitation source based on a frequency comb-emitting THz QCL [27]. By coupling the THz QCL FC to the tip of the s-SNOM, the intermode FC beatnote can be modulated in intensity, position and linewidth through optical feedback and used to drive the laser in a stable comb regime; the FC itself can be, in turn, used as a detector of the field backscattered by the nanoscope tip. Such coherent, detectorless FC nanoscope can provide nanoscale (40-100 nm) resolution at multiple THz frequencies over a continuous spectral bandwidth (2-5 THz), with fast acquisition rates (<ms/pixel) and pW/Hz$^{1/2}$ noise equivalent powers, simultaneously, solving the present hand-user limitations of commercial

Optical Materials EXPRESS

THz TDS s-SNOM apparatus. The combined nanoscale spatial resolution and phase-sensitive homodyne detection achievable with this technique prospects extensive opportunities in the 3-10 THz frequency range, for example for probing bio-samples over the nm scale or reconstructing the dispersion of photoexcited modes bio-samples.

4. Synthetic holography

Optical holography [28] is an imaging technique where the light scattered from an illuminated object is superposed with a reference wave. The resulting interference pattern—the hologram—encodes the complex optical field scattered from an object within a single image.

Synthetic optical holography (SOH) is a recently introduced holographic modality of quantitative phase imaging in s-SNOM [29]. While the sample is rapidly scanned in position, the reference mirror of the interferometer is slowly translated to modulate the phase of the reference field. An intriguing perspective is to take advantage of SMI to implement the same acquisition strategy in a compact detectorless configuration. Instead of measuring near field maps at fixed L, the optical path length, or the phase, at each pixel, can be varied while the s-SNOM is scanning the sample, hence reconstructing a hologram.

This technique can be an extremely powerful tool for measuring, in one shot, the dispersion characteristics of 2D nanomaterials, employing a coherent multiwavelength source as a QCL FC. It is also appealing for mapping the confined electromagnetic resonant modes in micro-resonators over larger scales (μm^2) still with nanoscale resolution or for imaging propagation of confined modes in the split gap of a resonators/metamaterials embedding a 2D material.

5. Aperture type near field nanoscopy

s-SNOM exploit an atomic force microscope (AFM) tip to induce strongly concentrated THz fields at the tip apex. A fraction of the concentrated field is scattered, and the scattered wave carries information about the dielectric constant ε underneath the tip in its amplitude and phase, therefore enabling spatial resolution determined by the tip apex size rather than the wavelength. However, the scattering efficiency of the AFM tip is prohibitively low in the THz frequency range. Conversely, the original near-field microscopy concept [30], relies on detecting light through a sub-wavelength aperture in a metallic screen. The spatial resolution of this method is determined by the aperture size (a), and it is usually adopted to probe structural characteristics over millimeter size samples.

The transmitted field also contains evanescent waves, which are localized in the near-field zone of the aperture [31]. These evanescent waves represent the major component of the transmitted field for deeply sub-wavelength apertures ($<\lambda/100$) [32]. However, being localized at the aperture, they remain almost undetected in most near-field imaging systems. A recently developed approach to overcome the issue is encoded in a novel near-field THz probe concept, where the evanescent THz field is converted into a detectable electrical signal at the nanoscale [33]. A THz nanodetector based on thin flake of bi-dimensional nanomaterials can be integrated into the evanescent field region of a sub-wavelength aperture to enable efficient detection of the transmitted wave (Fig. 1(b),(c)). To access the phase information from a detector, that, by design, is an inherently incoherent detector, one can propose a scheme (Fig. 1(d)), where the aperture probe is also back illuminated from the top side (Fig. 1(d)). This approach also allows to boost the sensitivity as we can use coherent gain and amplify even the weakest signal.

6. Photocurrent nanoscopy

Nanoscale-resolved THz photocurrent near-field microscopy is a technique in which near field signals associated with light-induced effects (as propagating modes or photocurrents) are detected

Optical Materials EXPRESS

thermoelectrically rather than optically [34]. This technique allows on-chip detection and simplifies imaging, as more sophisticated s-SNOM detection schemes can be avoided.

This technique, still making use of a thermally stable [35] THz QCL to photoexcite the sample, can be employed to investigate local photocurrents induced by illumination in one-dimensional (1D) nanostructures such as nanowires [5] (Fig. 1(e)), allowing reconstructing the different spatial distribution of the current profiles thought the photocurrent distribution (with nanoscale resolution) along the nanowire axis (Fig. 1(f)). This can be unambiguously identify the nature of the photoresponse (thermoelectric, bolometric, plasmonic) [36], hence allowing to engineer the detection speed, which, in a thermally driven THz photo-response, is limited by the efficiency of the energy transfer between incoming photons and the photo-detecting system. The same concept can be easily extended to 2D nanomaterials-based photodetectors, which actually outperform, in the THz, the performance of commercial detectors [37]. It can also be adopted to capture THz acoustic plasmons in graphene [5] (Fig. 1(f)), and offer potential challenges to trace deeply sub-wavelength THz plasmon polaritons ($\lambda_p \approx \lambda_0/100$), with dispersion tunable by electrostatic control of the carrier density. This is highly appealing in 2D anisotropic materials, since the in-plane anisotropy of the dielectric response can result into anisotropic polariton propagation. This could be innovatively exploited for inducing directional subwavelength light confinement.

Funding. HORIZON EUROPE European Research Council (101081567, 681379).

Disclosures. The authors declare that there are no conflicts of interest related to this article.

Data availability. The data provided in Fig. 1 are available upon reasonable request to the author.

References

1. A. J. L. Adam, "Review of near-field terahertz measurement methods and their applications," J. Infrared, Millimeter, Terahertz Waves **32**(8-9), 976–1019 (2011).
2. O. Mitrofanov, Y. Todorov, D. Gacemi, A. Mottaghizadeh, C. Sirtori, I. Brener, and J. L. Reno, "Near-field spectroscopy and tuning of sub-surface modes in plasmonic terahertz resonators," Opt. Express **26**(6), 7437–7450 (2018).
3. B. J. Bohn, M. Schnell, M. A. Kats, F. Aieta, R. Hillenbrand, and F. Capasso, "Near-field imaging of phased array metasurfaces," Nano Lett. **15**(6), 3851–3858 (2015).
4. Z. Li, S. Yan, Z. Zang, G. Geng, Z. Yang, J. Li, L. Wang, C. Yao, H.-L. Cui, C. Chang, and H. Wang, "Single cell imaging with near-field terahertz scanning microscopy," Cell Proliferation **53**, e12788 (2020).
5. E. A. A. Pogna, M. Asgari, V. Zannier, L. Sorba, L. Viti, and M. S. Vitiello, "Unveiling the detection dynamics of semiconductor nanowire photodetectors by terahertz near-field nanoscopy," Light: Sci. Appl. **9**(1), 189 (2020).
6. V. Iyer, Y. S. Phang, A. Butler, J. Chen, B. Lerner, C. Argyropoulos, T. Hoang, and B. Lawrie, "Near-field imaging of plasmonic nanopatch antennas with integrated semiconductor quantum dots," APL Photonics **6**(10), 106103 (2021).
7. Z. Fei, A. S. Rodin, and G. O. Andreev, *et al.*, "Gate-tuning of graphene plasmons revealed by infrared nano-imaging," Nature **487**(7405), 82–85 (2012).
8. J. Chen, M. Badioli, and P. Alonso-González, *et al.*, "Optical nano-imaging of gate-tunable graphene plasmons," Nature **487**(7405), 77–81 (2012).
9. G. X. Ni, L. Wang, and M. D. Goldflam, *et al.*, "Ultrafast optical switching of infrared plasmon polaritons in high-mobility graphene," Nat. Photonics **10**(4), 244–247 (2016).
10. S. Zhang, B. Li, and X. Chen, *et al.*, "Nano-spectroscopy of excitons in atomically thin transition metal dichalcogenides," Nat. Commun. **13**(1), 542 (2022).
11. S. Dai, Z. Fei, and Q. Ma, *et al.*, "Tunable phonon polaritons in atomically thin van der Waals crystals of boron nitride," Science **343**(6175), 1125–1129 (2014).
12. M. A. Huber, F. Mooshammer, and M. Plankl, *et al.*, "Femtosecond photo-switching of interface polaritons in black phosphorus heterostructures," Nat. Nanotechnol. **12**(3), 207–211 (2017).
13. N. A. Aghamiri, F. Huth, and A. J. Huber, *et al.*, "Hyperspectral time-domain terahertz nanoimaging Opt," Opt. Express **27**(17), 24231 (2019).
14. A. J. Huber, F. Keilmann, and J. Wittborn, *et al.*, "Terahertz near-field nanoscopy of mobile carriers in single semiconductor nanodevices," Nano Lett. **8**(11), 3766–3770 (2008).
15. F. Kuschewski, F. Kuschewski, and F. Kuschewski, *et al.*, "Narrow-band near-field nanoscopy in the spectral range from 1.3 to 8.5 THz," Appl. Phys. Lett. **108**(11), 113102 (2016).
16. C. Liewald, Hesler Mastel, and J. Jeffrey, *et al.*, "All-electronic terahertz nanoscopy," Optica **5**(2), 159–163 (2018).
17. M. Giordano, S. Mastel, and C. Liewald, *et al.*, "Phase-resolved THz self-detection near-field microscopy," Opt. Express **26**(14), 18423 (2018).
18. K. S. Reichel, E. A. Aurelia Pogna, and S. Biasco, *et al.*, "Self-mixing interferometry and near-field nanoscopy in quantum cascade random lasers at terahertz frequencies," Nanophotonics **10**(5), 1495–1503 (2021).

Optical Materials EXPRESS

19. E. A. A. Pogna, C. Silvestri, and L. L. Columbo, *et al.*, "Terahertz near-field nanoscopy based on detectorless laser feedback interferometry under different feedback regimes," APL Photonics **6**(6), 061302 (2021).
20. E. Riccardi, V. Pistore, L. Consolino, A. Sorgi, F. Cappelli, R. Eramo, P. De Natale, L. Li, G.A. Davies, E. H Linfield, and M. S. Vitiello, "Terahertz sources based on metrological-grade frequency comb," Laser Photonics Rev. **17**, 2200412 (2023).
21. G. Giuliani and S. Donati, "Laser interferometry," in *Unlocking Dynamical Diversity* (John Wiley & Sons, Ltd, 2005), pp. 217–255.
22. T. Taimre, M. Nikolić, K. Bertling, Y. L. Lim, T. Bosch, and A. D. Rakić, "Laser feedback interferometry: a tutorial on the self-mixing effect for coherent sensing," Adv. Opt. Photonics **7**(3), 570–631 (2015).
23. C. G. Derntl, G. Scalari, D. Bachmann, M. Beck, J. Faist, K. Unterrainer, and J. Darmo, "Gain dynamics in a heterogeneous terahertz quantum cascade laser," Appl. Phys. Lett. **113**(18), 181102 (2018).
24. R. Lang and K. Kobayashi, "External optical feedback effects on semiconductor injection laser properties," IEEE J. Quantum Electron. **16**(3), 347–355 (1980).
25. L. L. Columbo and M. Brambilla, "Multimode regimes in quantum cascade lasers with optical feedback," Opt. Express **22**(9), 10105–10118 (2014).
26. E. A. A. Pogna, L. Viti, A. Politano, M. Brambilla, G. Scamarcio, and M. S. Vitiellom, "Mapping propagation of collective modes in Bi_2Se_3 and $Bi_2Te_{2.2}Se_{0.8}$ topological insulators by near-field terahertz nanoscopy," Nat. Commun. **12**(1), 6672 (2021).
27. V. Pistore, E. A. A. Pogna, L. Viti, L. Li, A. G. Davies, E. H. Linfield, and M. S. Vitiello, "Self-induced phase locking of terahertz frequency combs in a phase-sensitive hyperspectral near-field nanoscope," Adv. Sci. **9**, 2200410 (2022).
28. P. Hariharan, *Optical Holography* (Cambridge University Press, 1996).
29. M. Schnell, P. S. Carney, and R. Hillenbrand, "Synthetic optical holography for rapid nanoimaging," Nat. Commun. **5**(1), 3499 (2014).
30. E. Ash and G. Nicholls, "Super-resolution aperture scanning microscope," Nature **237**(5357), 510–512 (1972).
31. C. G. Wade, N. Šibalić, and N. R. de Melo, *et al.*, "Real-time near-field terahertz imaging with atomic optical fluorescence," Nat. Photonics **11**(1), 40–43 (2017).
32. O. Mitrofanov, M. Lee, and J. W. P. Hsu, *et al.*, "Collection-mode near-field imaging with 0.5-THz pulses," IEEE J. Sel. Top. Quantum Electron. **7**(4), 600–607 (2001).
33. O. Mitrofanov, L. Viti, E. Dardanis, M. C. Giordano, D. Ercolani, A. Politano, L. Sorba, and M. S. Vitiello, "Near-field terahertz probes with room-temperature nanodetectors for subwavelength resolution imaging," Sci. Rep. **7**(1), 44240 (2017).
34. P. Alonso-González, A. Y. Nikitin, Y. Gao, A. Woessner, M. B. Lundeberg, A. Principi, N. Forcellini, W. Yan, S. Vélez, A. J. Huber, K. Watanabe, T. Taniguchi, F. Casanova, L. E. Hueso, M. Polini, J. Hone, F. H. L. Koppens, and R. Hillenbrand, "Acoustic terahertz graphene plasmons revealed by photocurrent nanoscopy," Nat. Nanotechnol. **12**(1), 31–35 (2017).
35. M. S Vitiello, G. Scamarcio, V. Spagnolo, J. Alton, S. Barbieri, C. Worrall, H. E Beere, D. A Ritchie, and C. Sirtori, "Thermal properties of THz quantum cascade lasers based on different optical waveguide configurations," Appl. Phys. Lett. **89**(2), 021111 (2006).
36. F. H. L. Koppens, T. Mueller, P. Avouris, A. C. Ferrari, M. Polini, and M. S. Vitiello, "Photodetectors based on graphene, other two-dimensional materials and hybrid systems," Nat. Nanotechnol. **9**(10), 780–793 (2014).
37. L. Viti, D. G. Purdie, A. Lombardo, A. C. Ferrari, and M. S. Vitiello, "HBN-encapsulated, graphene-based, room-temperature terahertz receivers, with high speed and low noise," Nano Lett. **20**(5), 3169–3177 (2020).